Prediction of double retrograde vaporization: transition in binary mixtures of near critical fluids with components of homologous series

S. Espinosa [a], S. Raeissi [b], E.A. Brignole [a], C.J. Peters [b,*]

[a] PLAPIQUI, Universidad Nacional del Sur—CONICET, CC 717, 8000 Bahía Blanca, Argentina
[b] Laboratory of Physical Chemistry and Molecular Thermodynamics, Faculty of Applied Sciences, DelftChemTech,
Delft University of Technology, Julianalaan 136, 2628 BL Delft, The Netherlands

Abstract

The phenomenon of double retrograde vaporization (DRV) has been simulated using the group contribution equation of state coupled with the Michelsen computational procedures for calculating phase envelopes. This behavior was studied for a number of binary mixtures of near critical fluids with a low volatile component. For the binary systems ethane + limonene, ethane + linalool, methane + butane, and methane + pentane the "double-domed" and "S" shaped curves were successfully predicted and found to be in good agreement with the experimental information available. Prediction of DRV in a number of binary systems from different families further confirmed the idea of the generality of this behavior in all asymmetric mixtures. All results indicate that as the solute increases in molecular size, the composition at which the phenomenon of DRV starts to appear shifts to higher solvent concentration, while simultaneously covering a wider composition range. For the homologous n-alkane series in binary mixtures with C_1 up to C_5 as near-critical solvents, a correlation in the appearance of the phenomenon of DRV with the hard-sphere diameter of the solvent was observed. Although for each solvent, the lower limit of solute carbon number that shows DRV is easily estimated, the upper carbon number could not always be determined because the occurrence of liquid–liquid immiscibility interferes with the DRV phenomenon. In binary mixtures of CO_2 with homologous members of alkyl esters, no liquid–liquid immiscibility was predicted, so it was possible to determine both the lower and upper concentration bounds of DRV.
© 2004 Elsevier B.V. All rights reserved.

1. Introduction

The challenging problems of the process industry in the current century have promoted extensive research in the field of supercritical fluid technology. However, any successful process design is dependent on accurate knowledge of thermodynamic properties. Although this is true in general for any type of process design, the understanding of phase behavior in supercritical processes is of even higher significance as the phase behavior near the critical region may exhibit extreme trends. This is in particular the case of highly diluted solute mixtures in a solvent at near-critical conditions. Under these conditions, it is likely that the mixture gives rise to the phenomenon that has been identified as double retrograde vaporization (DRV).

DRV occurs in mixtures having (high) molecular asymmetry (difference in size, shape and interaction energy between the solute and solvent molecules) and is characterized by an anomalous retrograde dew point curve at small solute concentrations and at temperatures close to the critical temperature T_{c_A}, of the solvent. On the P–x, y diagram, schematically shown in the far right side of Fig. 1a, instead of the single-domed dew point curve in the familiar "single" retrograde vaporization, DRV shows two "domes" at temperatures close to, but above T_{c_A}. In this case, quadruple-valued dew points are observed since a pressure decrease at constant composition and temperature will cause the following phase transitions to occur: vapor → vapor + liquid → vapor → vapor + liquid → vapor. At temperatures below but close to T_{c_A}, the dew point curve has an "S" shape as shown in the

* Corresponding author. Tel.: +31-15-2782660; fax: +31-15-2788668.
E-mail addresses: ebrignole@plapiqui.edu.ar (E.A. Brignole),
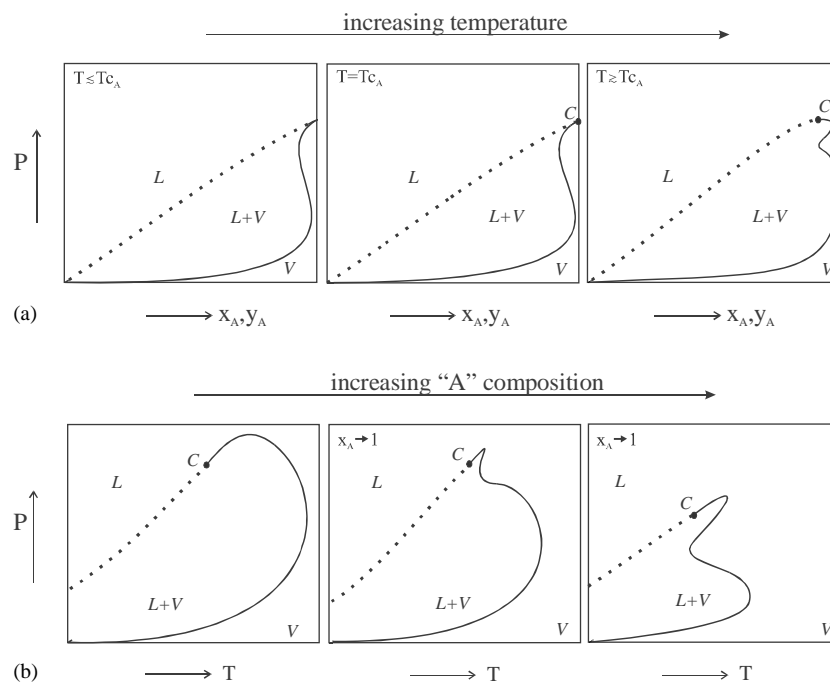cor.peters@tnw.tudelft.nl (C.J. Peters).

increasing temperature

(a)

increasing "A" composition

(b)

Fig. 1. Schematic presentation of double retrograde behavior on P–x, y and P–T coordinates. The dotted and solid curves indicate bubble and dew point curves respectively and the black dots are the critical points.

left side of Fig. 1a. This results in triple-valued dew point at a specific composition. Of course when P–x, y isotherms of a system show multiple dew point behavior, the P–T isopleths would also be characterized by multiple dew points (Fig. 1b). On such a diagram, DRV behavior can be found only within a certain composition range bounded by the two isopleths which have a vertical tangent to their critical and non-critical domes, as shown schematically in Fig. 2. For further details and explanations about DRV, see elsewhere [1].

DRV was observed experimentally by Chen et al. [2,3] for the systems methane + butane and methane + pentane. Raeissi and Peters [4] reviewed the previous work giving further experimental evidence of DRV. The studies attempting to simulate this phenomenon using equation of state

methods include the more recent work of Espinosa et al. [5], in addition to those listed by Raeissi and Peters [6]. After nearly three decades of neglect, a new phenomenological interest in DRV has given rise to explanations of the behavior and the description of the transitions of DRV with temperature on the P–x, y coordinates, and with composition on the P–T coordinates [1], in addition to the thermodynamic evaluation of the phenomenon [7,8].

In this study, we discussed additional characteristics of this phenomenon. The work is divided into two stages:

- First, the use of the group contribution equation of state (GC-EOS) in predicting DRV behavior is justified by comparing simulation results with the available experimental data in literature.
- Second, the trend of appearance and growth of DRV through homologous series of n-alkanes and alkyl esters with several supercritical solvents is investigated.
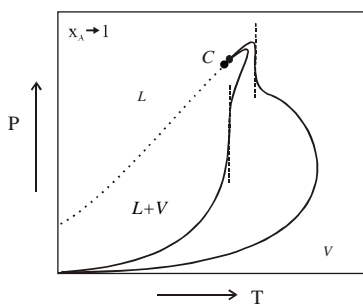

Fig. 2. Schematic presentation of the two isopleths with the minimum and maximum mole fractions, respectively, at which DRV behavior can be observed. The dotted and solid curves indicate bubble and dew point curves respectively and the black dots are the critical points of the two isopleths.

2. Vapor–liquid equilibria predictions

The phase boundary for DRV shows sharp changes in slope in the vicinity of the critical point of component A and, therefore, a robust computational procedure is required to obtain reliable predictions of phase equilibria in this region. In this case, the numerical procedure of Michelsen [9] for phase envelope calculations coupled with the GC-EOS thermodynamic model by Skjold-Jorgensen [10] was applied.

The basis of the GC-EOS is the generalized van der Waals partition function combined with the local composition principle. The residual Helmholtz function is divided into an attractive and a free volume term. The free volume part is described by an expression for hard spheres, while the attractive part is a group contribution version of a density dependent NRTL type expression [11]. For details of the equation of state and its derived relations, see elsewhere [10].

Predictions with the GC-EOS require a number of pure group and binary group interaction parameters. With the exception of the alcohol group of linalool, in the present study all predictions were based on the original parameter tables of Skjold-Jorgensen [10], the additional pure group and binary interaction parameters for olefinic groups by Push and Schmelzer [11], the improved binary interaction parameters between CO_2 and paraffins by Espinosa et al. [12], and the CO_2 and aromatic groups presented by Bamberger et al. [13]. The proximity effects in linalool, due to the presence of the tertiary alcohol group close to an olefinic group, made it necessary to include a special binary interaction parameter between this group with ethane. This parameter was obtained on the basis of the experimental data reported by Raeissi et al. [14] for the system ethane + linalool. For further details and the parameter values, see elsewhere [5].

3. GC-EOS capability in simulating experimental DRV data

There is a serious lack of experimental DRV data in literature. The following binary VLE data have been simulated in this work: ethane + limonene [15] and ethane + linalool [1] in the form of P–T isopleths, and methane + butane [2] and methane + pentane [3] as P–x, y isotherms. The GC-EOS proved to be successful in simulating DRV behavior in all these systems, not only qualitatively but also quantitatively. This can be seen, for example, for ethane+linalool in Fig. 3. The phase envelope for the ethane + linalool system at 99.98 mol% ethane particularly illustrates the robustness of the Michelsen procedure in representing very sharp changes in the phase envelope in the critical region of the mixture. The general trend of appearance and growth of DRV is clearly apparent by proceeding through the different plots in Fig. 3, with the characteristic growth of the "critical dome" and simultaneous shrinkage of the "non-critical dome" as the mixture approaches closer and closer to the pure solvent. Similar comparisons for ethane + limonene have already been presented in an earlier work [5].

On different space coordinates, the comparison between predictions and data for methane + butane and methane + pentane also indicate the good predicting capability as shown in Figs. 4 and 5, especially by considering the scale of the
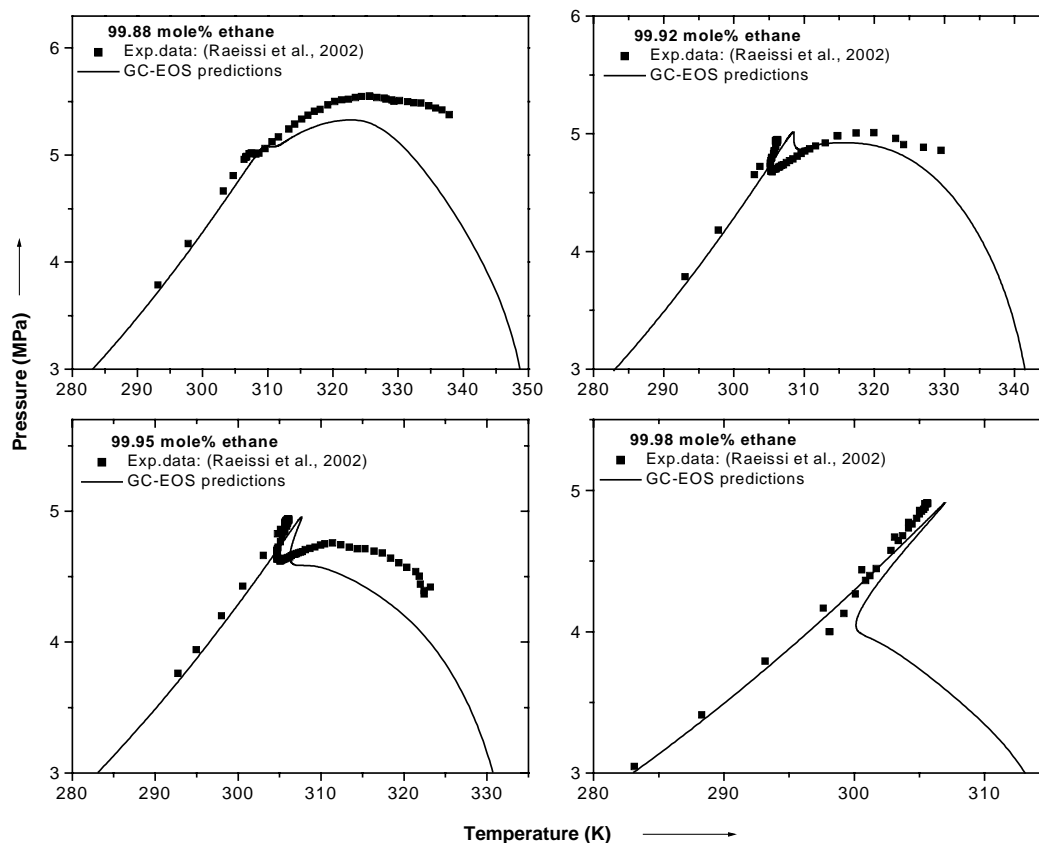

Fig. 3. Comparison of GC-EOS predictions with the experimental bubble and dew point data for four isopleths of the system ethane + linalool [1].
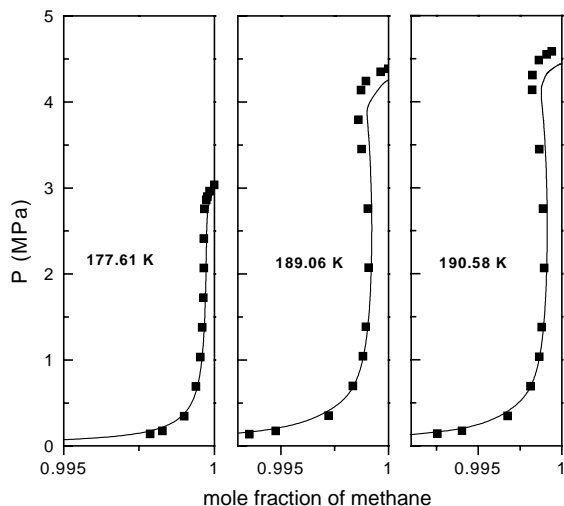
Fig. 4. Comparison of GC-EOS predictions of DRV (continuous curve) with the experimental dew point data of Chen et al. [2] (points) for three isotherms of the system methane + butane.
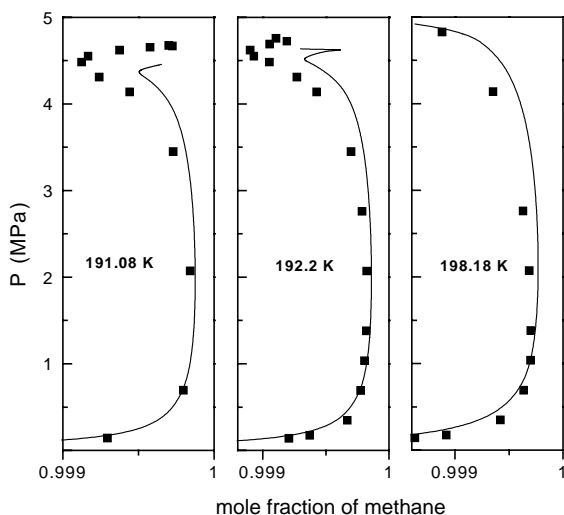

Fig. 5. Comparison of GC-EOS predictions of DRV (continuous curve) with the experimental dew point data of Chen et al. [3] (points) for three isotherms of the system methane + pentane.

x-axis. Methane+butane exhibits the triple-valued dew point characteristics for temperatures below the critical temperature of the solvent, while methane + pentane exhibits the full double-domed DRV behavior at temperatures above the solvent critical point.

4. Appearance and trends of DRV behavior in homologous series

Considering the adequate performance of the GC-EOS in predicting DRV behavior, the phenomenon was further investigated, based on the group contribution equation approach to predict the appearance and trend of change in the
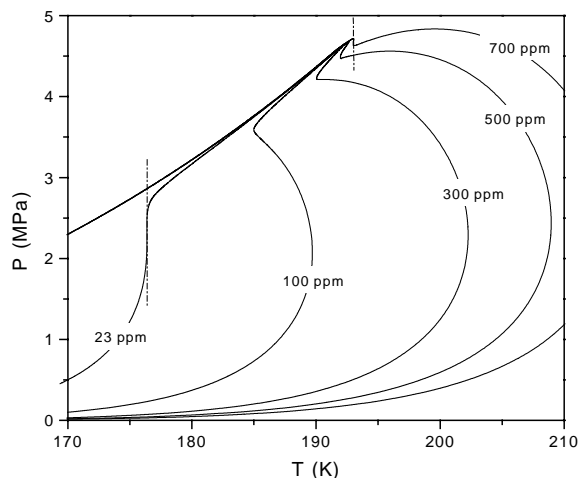

Fig. 6. GC-EOS predictions of DRV for binary mixtures of methane+ pentane at different concentrations (in ppm of pentane), including the lower and upper concentration boundaries of DRV (23 and 700 ppm, respectively).

shape and range of DRV in binary mixtures of near-critical fluids with components belonging to homologous series.

4.1. n-Alkane + n-alkane homologous series

A selected number of homologous n-alkane mixtures have been chosen in order to investigate their near-critical phase behavior. The solvents range from methane up to pentane, while the solutes go up to as high as octacosane.

4.1.1. Methane + n-alkanes

As an example, Fig. 6 illustrates P–T coordinate DRV plots in binary mixtures of methane + pentane for five different isopleths. Comparison of this system with experimental data was previously discussed in Section 3. Fig. 6 also exhibits two concentrations (700 and 23 ppm pentane, respectively) at which the critical and non-critical domes have vertical tangents (dashed lines on figure). Such limiting isopleths indicate the beginning and end of the DRV phenomenon for a given binary system. In other words, DRV behavior appears, grows, and diminishes within the small range of compositions bounded by these two isopleths.

Fig. 7 shows the shapes of the DRV dew curves for three members of the homologous n-alkane series in methane. As the carbon number increases, DRV begins to appear at smaller solute concentrations. This is also in agreement with previously observed experimental data on binary systems of limonene and linalool with ethane [1]. Linalool with a molecular mass of 154.25 g/mol does not yet show any DRV behavior at a concentration of 99.79 mol% ethane, while, at exactly the same concentration of 99.79 mol.% ethane, limonene having a molecular mass of 136.24 g/mol has already begun to form a dent in the dew point curve characteristic for DRV.
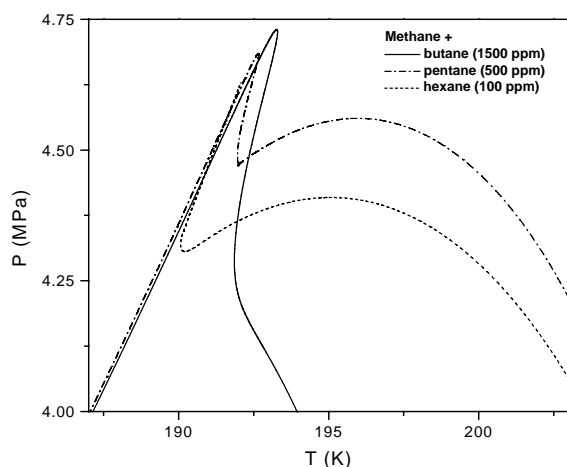
Fig. 7. GC-EOS predictions of DRV for binary systems of methane with some members of the homologous *n*-alkane series.

Fig. 9. GC-EOS predictions of DRV for binary systems of ethane with some members of the homologous *n*-alkane series.

It was found, however, that with successively heavier members of the homologous series, a point is reached where the predictions show instabilities, i.e., in this case for a six carbon number solute (hexane) with methane. The authors ascribe such instabilities to the occurrence of the well-known phenomenon [16] of three-phase liquid–liquid–vapor ($L_1 + L_2 + V$) equilibrium in the same region, which interferes with the phase envelope calculations. Fig. 8a illustrates the equilibrium regions for the system at 188.3 K. Although the GC-EOS estimates are hindered by computational instabilities, in fact it is possible that the liquid–liquid immiscibility and DRV can couple together to form the interesting case shown in Fig. 8b, with the following sequence of phase transitions upon increasing pressure at constant composition: $V \rightarrow V + L_1 \rightarrow V \rightarrow V + L_2 \rightarrow L_2$. It must be noted that the GC-EOS qualitatively, be it not quantitatively, predicts the existence of liquid–liquid immiscibility as well as
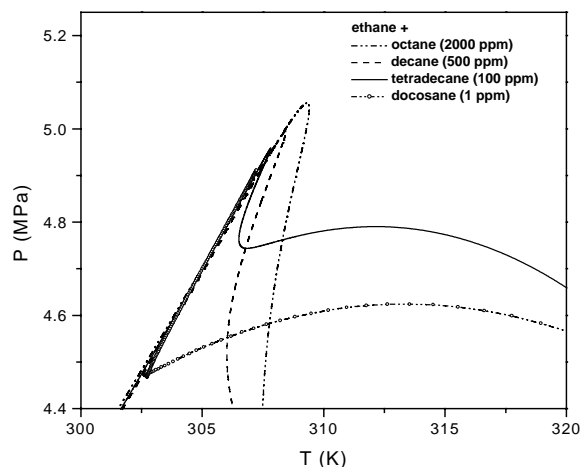
the extension of the three-phase locus, in accordance with experimental data [17].

4.1.2. Ethane + n-alkanes

A similar study was carried out for mixtures of *n*-alkanes with near-critical ethane. As a first step to check the predicting capability of the GC-EOS for such systems, the general phase behavior over wide composition ranges, not involving DRV, were also compared with experimental data for the binary systems of ethane with decane and eicosane. The results, not presented here, for the sake of brevity, indicate good agreement between predictions and experimental data. Then, focusing on the particular region of DRV, the phenomenon was predicted starting with octane and going up to docosane. Some of these estimations are plotted in Fig. 9. Octadecane was the first alkane to show interference of the three-phase equilibrium $L_1 + L_2 + V$ with the predicted DRV
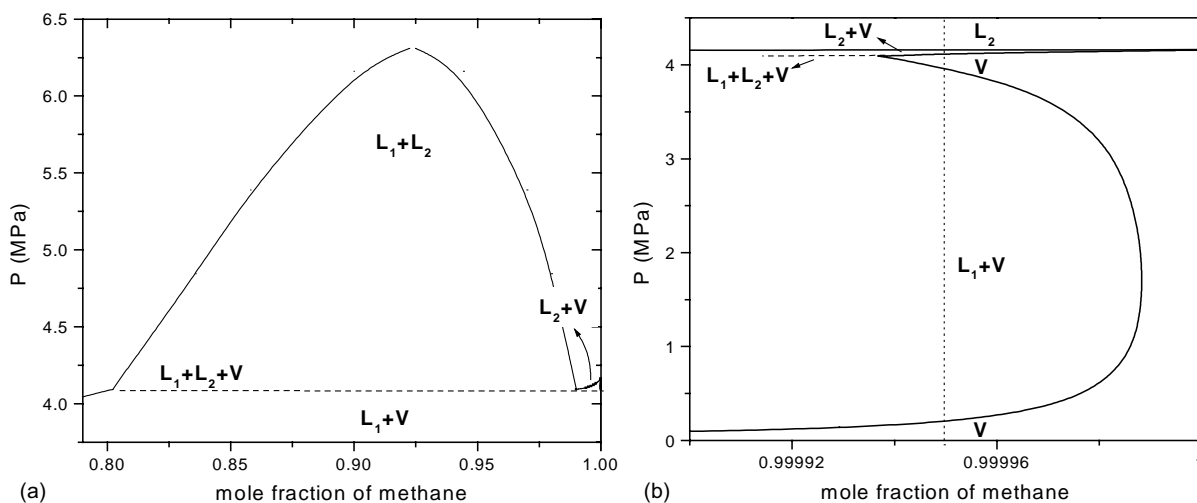

Fig. 8. DRV coupled with liquid–liquid immiscibility for the system methane + hexane: (a) *Pxy* GC-EOS predictions at 188.3 K; (b) phase transitions of both liquid–liquid immiscibility and double retrograde vaporization predicted for 188.3 K.
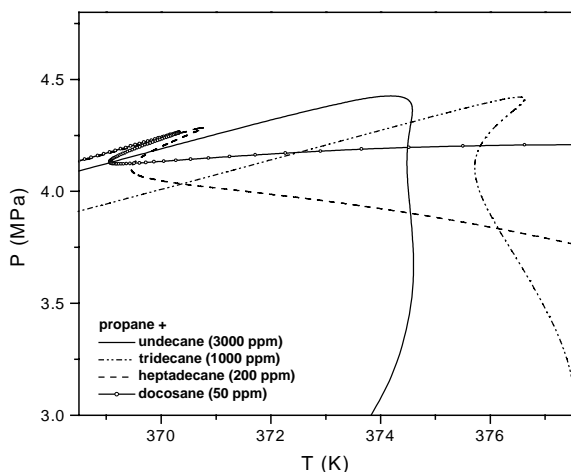
Fig. 10. GC-EOS predictions of DRV for binary systems of propane with some members of the homologous *n*-alkane series.

Fig. 11. Relationship between the hard-sphere diameters of the solvent and the most volatile solute at which DRV just starts to form.

in this system. The occurrence of a LLV equilibrium for this system is in agreement with the experimental observations of Pegg et al. [18].

4.1.3. Propane + n-alkanes

The systems of binary mixtures of near critical propane with *n*-alkanes were predicted to show DRV behavior within the range of undecane up to octacosane (Fig. 10).

4.1.4. Butane + n-alkanes

GC-EOS predictions for binary mixtures with butane as the near-critical component indicate heptadecane to be the first *n*-alkane to exhibit DRV with butane.

4.1.5. Pentane + n-alkanes

Nonadecane is the first *n*-alkane to exhibit DRV in combination with pentane.

4.1.6. Generalization for n-alkane homologues

In studies involving homologous series, it is a common approach to establish general relationships based on carbon numbers. However, in the GC-EOS, members of homologous series are not identified by carbon numbers, but rather by their hard-sphere diameters as given by the Carnahan–Starling expression. The results for *n*-alkane + *n*-alkane homologues (Fig. 11), do indeed indicate a correlation between the hard-sphere diameters of the solvent and the most volatile solute at which the DRV phenomenon begins, at least within the range of solvents from C_1 to C_5. Of course, taking into account the discrete character of properties of members of homologous series, one cannot expect a perfectly linear relationship to prevail. For example, in combination with ethane as the solvent, octane is the first *n*-alkane member to show DRV, which seems to be a too large *n*-alkane member for a perfectly linear fit according to Fig. 11. However, the next lower member in the homologous series, heptane, is a too small *n*-alkane to fit
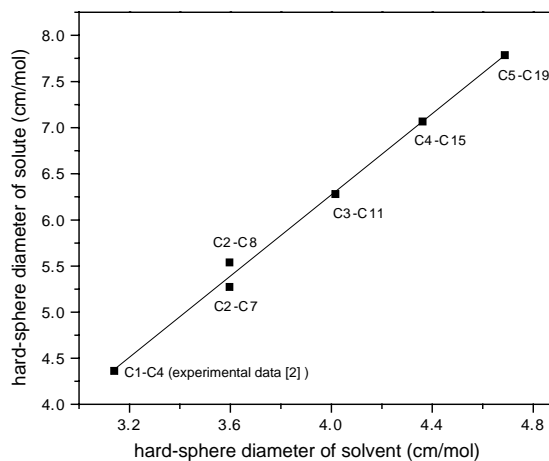
exactly the linear correlation of Fig. 11. In addition, there is also the issue of uncertainties and errors in the values of hard-sphere diameters, which can also contribute to some scattering in the perfectly linear fit.

The major conclusions from the homologous *n*-alkane series are summarized as follows:

1. DRV behavior was predicted in all the homologous series investigated within specific concentration ranges. This further supports the idea [1,5,6] that DRV is a common phenomenon in asymmetrical systems.
2. In principle, the heavier the solute, the higher the solvent concentration required to observe double retrograde behavior in such binary mixtures.
3. In the range of solvents from C_1 to C_5, there is a reasonably linear relationship between the hard-sphere diameters of the solvent and the most volatile solute at which the DRV phenomenon just starts to take place. This trend may well continue to higher members of the *n*-alkane homologous family.
4. The upper limit of *n*-alkane carbon numbers showing DRV could not be determined due to the occurrence of three-phase equilibria LLV.

4.2. Carbon dioxide + n-alkanes

Mixtures of carbon dioxide with members of the *n*-alkane homologous series show similar behavior and trends compared to the *n*-alkane systems as discussed above. The necessary asymmetry for the existence of DRV is not associated alone with the size of the compounds, but also with their interactions. Carbon dioxide starts to show DRV for the first time with hexane and continues up to tetradecane. Although binary mixtures of carbon dioxide with *n*-alkanes show already liquid–liquid immiscibility at significantly lower carbon numbers than that of hexadecane [16], nevertheless, the binary system of carbon dioxide with hexadecane was the first system showing the instabilities characteristic for the
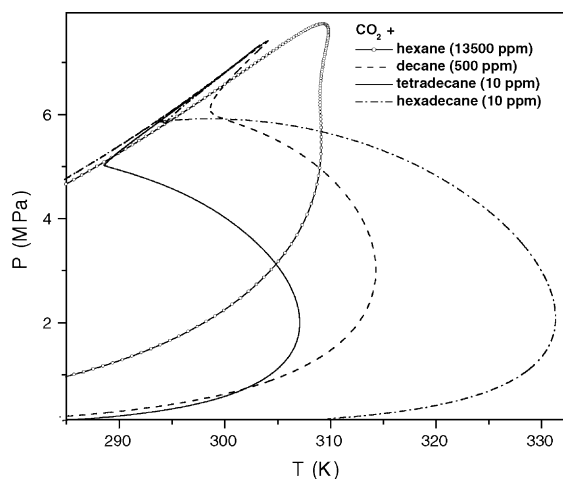
Fig. 12. GC-EOS predictions of DRV for binary systems of carbon dioxide and some members of the homologous *n*-alkane series.
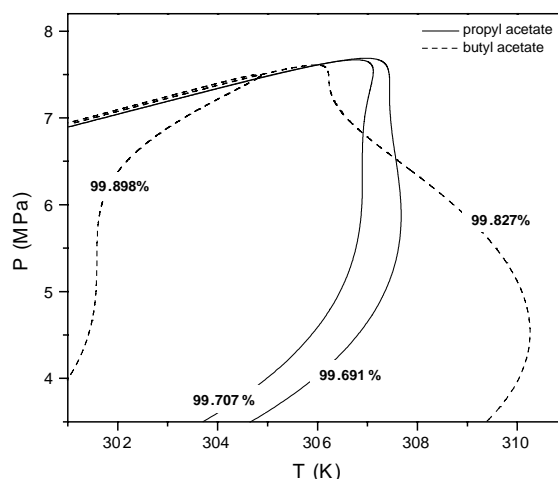

Fig. 13. GC-EOS predictions of DRV for binary systems of carbon dioxide and two different alkyl-acetate family members. For each binary system, the two extreme concentrations (in mol% of carbon dioxide) are plotted, corresponding to the boundaries of appearance and disappearance of DRV.

presence of liquid–liquid immiscibility. Some examples of the shapes and trends of DRV in these binary systems are shown in Fig. 12.

4.3. Carbon dioxide + alkyl esters

A number of binary mixtures of carbon dioxide with different members within the same homologous family, and also with different ester families have been investigated.

4.3.1. Changes in the alkyl chain size

Going through the family members with different alkyl groups within the same ester family, one finds similar trends compared to those observed for the *n*-alkane homologues. A certain chain-length is necessary to produce DRV. The limiting alkyl group sizes required are indicated in Table 1 for a selection of alkyl esters. Fig. 13 presents a plot of DRV behavior and its concentration boundaries for two acetate family members. It is interesting to note how the DRV behavior is more pronounced as the solute chain size

increases. Fig. 14 gives an even clearer view of the growth of the DRV concentration range as chain size, and hence molecular asymmetry increases.

4.3.2. Changes in the ester chain size

Considering alkyl ester family members of progressively increasing ester group size, the predictions of the GC-EOS would imply that it is not so much the size of the ester group itself rather than it is the whole molecule size that determines the occurrence of DRV. This can be seen in Table 1 for propyl acetate, ethyl propionate, and methyl butyrate. A DRV plot is also shown for these different ester families in Fig. 15. These limiting components, marking the beginning of DRV behavior come from different ester families but all have the same molecular mass of 102.13 g/mol and consist of the same atoms, although positioned differently in the molecule. This may be attributed to the general limitation of the group contribution methods in quantifying interactions of the same groups in different positions.

Table 1
Ranges of existence of DRV for alkyl esters with carbon dioxide as predicted by the GC-EOS

| Ester family	Alkyl ester	Molar mass (g/mol)	Hard-sphere diameter (cm/mol)	Existence of DRV	Lower concentration range of DRV in mole fraction	Upper concentration range of DRV in mole fraction
Acetates	Methyl acetate	74.08	4.7532	No	–	–
	Ethyl acetate	88.11	5.0996	No	–	–
	Propyl acetate	102.13	5.3801	Yes	99.691	99.707
	Butyl acetate	116.16	5.6332	Yes	99.827	99.898
Propionates	Methyl propionate	88.11	4.8529	No	–	–
	Ethyl propionate	102.13	5.2016	Yes	99.672	99.695
	Propyl propionate	116.16	5.4773	Yes	99.811	99.889
Butyrates	Methyl butyrate	102.13	5.1684	Yes	99.704	99.748
	Ethyl butyrate	116.16	5.4962	Yes	99.804	99.877
	Propyl butyrate	130.19	5.7688	Yes	99.870	99.954
	Butyl butyrate	144.21	6.0767	Yes	99.900	99.976
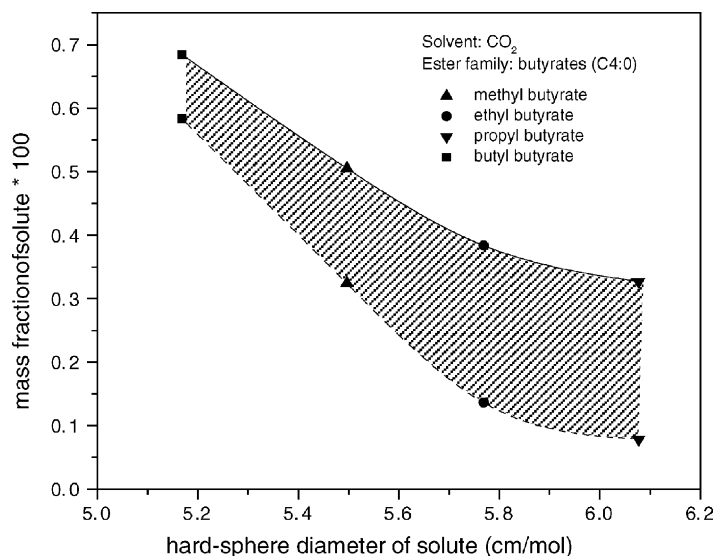
Fig. 14. Effect of chain length on the DRV behavior of binary systems of carbon dioxide and different butyrate family members. The solid and dashed curves represent the upper and lower concentration boundaries of DRV, respectively, and the region in between indicates the range of solute compositions with DRV.

4.3.3. Generalization for the alkyl ester-homologues

The results generally confirm those obtained with the n-alkane + n-alkane homologous series. One main difference however is that the alkyl ester binary mixtures with carbon dioxide exhibit a wider pressure range for DRV than previously observed in other systems. This may be a hopeful hint for the possibility of employing the phenomenon of DRV for practical purposes, such as separations.

Another difference is that in contrast to n-alkanes, the alkyl esters do not show any liquid–liquid immiscibility in the range of DRV, so it is easily possible to determine both the lower and upper concentration bounds of DRV. As the solute increases in molecular mass, both the minimum and maximum solvent concentrations required to produce DRV

shift to higher solvent concentrations, also increasing in concentration range (Table 1 and Fig. 14).

5. Conclusions

DRV is expected to arise in systems with (high) molecular asymmetry near the critical temperature of the more volatile component. A number of different binary mixtures were investigated and the GC-EOS was capable of predicting this phenomenon in every system that went beyond a given molecular asymmetry. These predictions confirmed the idea that DRV is a common phenomenon to all such systems. Consequently, the model was used to compare predictions with experimental results showing good agreement with available experimental data.

Investigations of n-alkane + n-alkane, CO_2 + n-alkane, and CO_2 + alkyl ester homologous series indicated that as the solute increases in chain length, DRV occurs at progressively higher solvent concentrations. This may well be the general trend for all homologous series. This direct relation between DRV solvent concentration and solute–solvent asymmetry has also been observed experimentally for two binary mixtures of citrus oil constituents [1].

There is also a possibility that within certain concentration ranges, the phenomenon of DRV occurs simultaneously with liquid–liquid immiscibility to produce fascinating combinations of phase transitions as a function of pressure changes.

The investigation within homologous n-alkane + n-alkane series indicated that there is a linear relationship between the hard-sphere diameter of the solvent and the minimum solute hard-sphere diameter at which DRV begins to appear. Mixtures of alkyl ester family members with CO_2 indicated molecular size to be the major playing factor in determining
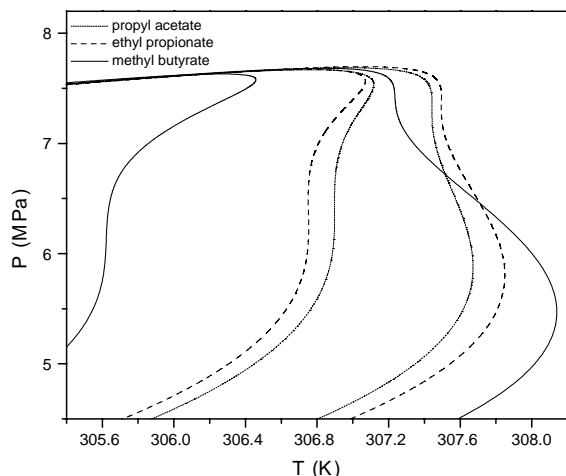

Fig. 15. GC-EOS predictions of DRV for binary systems of carbon dioxide and some different ester families. For each binary system, the two extreme concentrations corresponding to the boundaries of appearance and disappearance of DRV, as given in Table 1, are plotted.

the bounds of DRV in such systems, while the attractive interaction energies seem to be responsible for the range of compositions in which the phenomenon is present for each binary system.

References

[1] S. Raeissi, C.J. Peters, Double retrograde vaporization in the binary system ethane + linalool, J. Supercrit. Fluids 23 (2002) 1.

[2] R.J.J. Chen, P.S. Chappelear, R. Kobayashi, Dew point loci for methane-*n*-butane binary system, J. Chem. Eng. Data 19 (1974) 53.

[3] R.J.J. Chen, P.S. Chappelear, R. Kobayashi, Dew point loci for methane–*n*-pentane binary system, J. Chem. Eng. Data 19 (1974) 58.

[4] S. Raeissi, C.J. Peters, Double retrograde vaporization in a multi-component system: ethane + orange peel oil, J. Supercrit. Fluids, in press.

[5] S. Espinosa, S. Raeissi, E.A. Brignole, C.J. Peters, Prediction of the phenomenon of double retrograde vaporization using equation of state, in: Proceedings of the VIth Iberoamerican Conference on Phase Equilibria and Fluid Properties for Process Design, Iguazu Falls, Brazil, 12–16 October 2002.

[6] S. Raeissi, C.J. Peters, Simulation of double retrograde vaporization using the Peng–Robinson equation of state, J. Chem. Thermodyn. 35 (2003) 573.

[7] U.K. Deiters, Some comments on the double retrograde vaporization, J. Chem. Thermodyn. 35 (2003) 583.

[8] S. Raeissi, C.J. Peters, Thermodynamic analysis of the phenomenon of double retrograde vaporisation, in preparation.

[9] M.L. Michelsen, The isothermal flash problem. Part II. Phase-split calculation, Fluid Phase Equilib. 9 (1982) 21.

[10] S. Skjold-Jorgensen, Group contribution equation of state (GC-EOS): a predictive method for phase equilibrium computations over wide ranges of temperatures and pressures up to 30 MPa, Ind. Eng. Chem. Res. 27 (1988) 110.

[11] J. Pusch, J. Schmelzer, Extension of the group-contribution equation of state parameter matrix for the prediction of phase equilibria containing argon, ammonia, propene and other alkenes, Ber. Bunsenges. Phys. Chem. 97 (1993) 597.

[12] S. Espinosa, A. Bermúdez, G. Foco, T. Fornari, Revision and extension of the group contribution equation of state to new solvent groups and higher molecular weight alkanes, Fluid Phase Equilib. 172 (2000) 129.

[13] A. Bamberger, J. Schmelzer, D. Walther, G. Maurer, High-pressure vapor–liquid equilibria in binary mixtures of carbon dioxide and benzene compounds and their correlation with the generalized Bender and Skjold-Jorgensen's group contribution equation of state, Fluid Phase Equilib. 97 (1994) 167.

[14] S. Raeissi, J.C. Asensi, C.J. Peters, Phase behavior of the binary system ethane + linalool, J. Supercrit. Fluids 24 (2002) 111.

[15] S. Raeissi, C.J. Peters, On the phenomenon of double retrograde vaporization: multi dew point behavior in the binary system ethane + limonene, Fluid Phase Equilib. 191 (2001) 33.

[16] M.M. Miller, K.D. Luks, Observations on the multiphase equilibria behavior of CO_2-rich and ethane-rich mixtures, Fluid Phase Equilib. 44 (1989) 295.

[17] Y.N. Lin, R.J.J. Chen, P.S. Chappelear, R. Kobayashi, Vapor–liquid equilibria of the methane-hexane system at low temperature, J. Chem. Eng. Data 22 (1977) 402.

[18] L.L. Pegg, C.M. Knobler, R.L. Scott, Tricritical phenomena in quasi-binary mixtures. VIII. Calculations from the van der Waals equation for binary mixtures, J. Chem. Phys. 92 (1990) 5442.